Stopped-Flow Analysis of Substrate Binding to Neuronal Nitric Oxide Synthase†

Husam M. Abu-Soud,*,‡ Jianling Wang,§ Denis L. Rousseau,§ and Dennis J. Stuehr*,‡

Department of Immunology, NB-3, Lerner Research Institute, Cleveland Clinic Foundation, 9500 Euclid Avenue, Cleveland, Ohio 44195, and Department of Physiology and Biophysics, Albert Einstein College of Medicine, Bronx, New York 10461

Received March 25, 1999; Revised Manuscript Received June 22, 1999

ABSTRACT: The kinetics of binding L-arginine and three alternative substrates (homoarginine, *N*-methylarginine, and *N*-hydroxyarginine) to neuronal nitric oxide synthase (nNOS) were characterized by conventional and stopped-flow spectroscopy. Because binding these substrates has only a small effect on the light absorbance spectrum of tetrahydrobiopterin-saturated nNOS, their binding was monitored by following displacement of imidazole, which displays a significant change in Soret absorbance from 427 to 398 nm. Rates of spectral change upon mixing Im-nNOS with increasing amounts of substrates were obtained and found to be monophasic in all cases. For each substrate, a plot of the apparent rate versus substrate concentration showed saturation at the higher concentrations. K_{-1}, k_2, k_{-2}, and the apparent dissociation constant were derived for each substrate from the kinetic data. The dissociation constants mostly agreed with those calculated from equilibrium spectral data obtained by titrating Im-nNOS with each substrate. We conclude that nNOS follows a two-step, reversible mechanism of substrate binding in which there is a rapid equilibrium between Im-nNOS and the substrate S followed by a slower isomerization process to generate nNOS′−S: Im−nNOS + S ⇔ Im−nNOS−S ⇔ nNOS′−S + Im. All four substrates followed this general mechanism, but differences in their kinetic values were significant and may contribute to their varying capacities to support NO synthesis.

Nitric oxide (NO)[1] is an ubiquitous signal molecule that functions in the cardiovascular, nervous, and immune systems (*1*−*4*). Animals express three NO synthase isozymes (NOSs) that are homodimeric in their active forms and contain FAD, FMN, tetrahydrobiopterin (H_4biopterin), and iron protoporphyrin IX (heme) prosthetic groups. The NOSs catalyze a two-step oxidation of L-arginine (Arg) to generate NO plus L-citrulline, with *N*-hydroxy-L-arginine (NOHArg) being formed as an enzyme-bound intermediate. The heme iron plays a central role in catalysis by accepting NADPH-derived electrons from the NOS reductase domain, binding O_2 at both steps in the reaction, and activating it for incorporation into Arg and into NOHArg (*5*−*11*). Thus, consecutive heme-catalyzed monooxygenase reactions lead to oxygen incorporation into the NO and citrulline products (*5*, *12*). The proximal axial ligand for the NOS heme iron is a cysteine thiolate, as in the case for cytochrome P450s, and in the presence of bound substrate the ferric NOS heme iron is predominantly five-coordinate and high-spin (*6*, *7*, *13*).

Because binding Arg is an essential event in NO synthesis, understanding the NOS−substrate interaction in greater detail is important for elucidating the enzyme kinetic mechanism and possibly for developing highly selective inhibitors. Crystallographic data with substrate-bound NOSs indicates a funnel-shaped substrate binding channel that leads to the distal heme pocket, where a conserved glutamate residue holds the guanidinium group of Arg in place above the heme iron (*14*−*16*). The close proximity between heme and substrate as determined by crystallography is consistent with EPR, resonance Raman, and light absorbance spectral data that showed Arg influences heme iron electronic properties (*17*), reduction potential (*18*), and ligand binding properties (*19*−*26*) and causes expulsion of bulky heme iron ligands such as imidazole or DTT (*23*, *27*−*29*).

A variety of data suggest that the three NOS isozymes differ somewhat in their substrate binding properties (*22*, *30*). For example, only in neuronal NOS (nNOS) is Arg binding affinity independent of imidazole concentration (*22*, *23*). When Arg binds to imidazole-bound nNOS (Im−nNOS), the bound imidazole is expelled from the heme iron with an accompanying shift in Soret absorbance from 427 to 398 nm. The spectral change associated with this process has been used to quantitate Arg binding affinity in nNOS (*21*). Here, we utilized both equilibrium and stopped-flow spectroscopy to study the kinetics of substrate binding to Im−nNOS. We assumed that the binding kinetics remain the same in the presence and absence of imidazole, although this assumption was not directly tested in the current report.[2] Substrates examined include Arg, NOHArg, *N*-methyl-L-

† This work was supported by National Institutes of Health Grant GM51491 to D.J.S. and a grant from the American Heart Association to H.A.S. D.J.S. is an Established Investigator of the American Heart Association.

* To whom correspondence should be addressed. Fax: (216) 444-9329. E-mail: stuehrd@ccf.org; abusouh@ccf.org.

‡ Lerner Research Institute.

§ Albert Einstein College of Medicine.

[1] Abbreviations: Arg, L-arginine; H4biopterin, (6*R*,*S*)-5,6,7,8-tetrahydro-L-biopterin; homoArg, homo-L-arginine; Im-nNOS, imidazole-bound nNOS; NMA, *N*-methyl-L-arginine; nNOS, rat neuronal NOS; NO, nitric oxide; NOHArg, *N*-hydroxy-L-arginine; NOS, NO synthase.

10.1021/bi990698x CCC: $18.00
Published on Web 08/27/1999

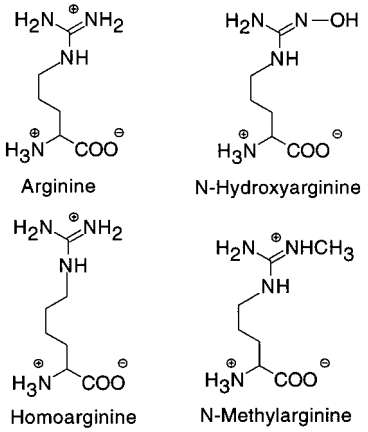

FIGURE 1: Structures of substrates used in this study.

arginine (NMA), and L-homoarginine (homoArg) (Figure 1). Together, our results provide a kinetic model for substrate binding to nNOS.

MATERIALS AND METHODS

Reagents. Human kidney cells expressing cloned rat brain nNOS were a kind gift of Drs. Solomon Snyder and David Bredt. All other reagents and materials were obtained from Sigma, Alexis, or from sources previously reported (*19*).

Cell Culture and Enzyme Purification. Kidney cells expressing nNOS were grown in 3 L spinner flasks in Dulbecco's modified Eagle medium supplemented with F-12 nutrient mixture (Gibco) containing 10% calf serum (Gibco), at 37 °C and 5% CO_2. Cells were harvested by centrifugation after reaching a density of $(1-2) \times 10^6$ cells/mL. The nNOS was purified from cell supernatants in the continuous presence of H_4biopterin, using a dual-column procedure and a Pharmacia FPLC as previously described (*9*, *10*). Column fractions containing purified nNOS were concentrated in centricon-30 microconcentrators (Amicon, Danvers, MA) at 4 °C and stored in 50 mL aliquots at −70 °C in 20 mM Bis-Tris propane buffer, pH 7.6, containing 3 mM DTT, 10% glycerol, and 2 μM each of FAD and H_4biopterin. The nNOS was ~90% pure as judged by SDS−PAGE, with specific activities that ranged between 500 and 850 nmol of NO formed/min per mg of protein at 37 °C, in good agreement with previous results (*8*−*11*). Protein content was assayed with the BioRad kit, using bovine serum albumin as a standard.

Measurement of NO Synthesis. The initial rate of NO synthesis by nNOS was quantitated at 37 °C using the oxyhemoglobin assay for NO as described previously (*8*−*11*). nNOS (0.5 μg) was added to a cuvette containing 40 mM Tris buffer, pH 7.8, supplemented with 5−10 μM oxyhemoglobin, 0.3 mM DTT, 1 mM Arg (or an alternative substrate), 0.1 mM NADPH, 4 μM each of FAD, FMN, and H_4biopterin, 100 units/mL of catalase, 10 units/mL of superoxide dismutase, and 0.1 mg/mL of bovine serum albumin, to give a final volume of 0.7 mL. The NO-mediated conversion of oxyhemoglobin to methemoglobin was monitored over time as an absorbance increase at 401 nm and quantitated using an extinction coefficient of 38 mM^{-1} cm^{-1}. To derive K_m values, substrate concentrations were varied from 3 μM to 5 mM, and double reciprocal velocity versus substrate concentration curves were used to estimate K_m.

Optical Spectroscopy. Spectra were recorded with a Hitachi 3110 spectrophotometer, at 15 °C, in Bis-Tris propane buffer pH 7.6. Titration experiments were performed with a 1 mL sample containing nNOS (0.7−1 μM), 1 mM imidazole, 1 mM DTT, and 4 μM H_4biopterin. Concentrated volumes of Arg solution or analogues were added consecutively to the sample cuvette, and absorbance changes were recorded from 300 to 700 nm after each addition. Difference spectra were obtained by subtracting the spectrum collected after each addition of substrate from that collected before the addition of substrate. The substrate spectral binding constant, K_s, was determined from the *x*-intercept of a double reciprocal plot of the difference in the respective peak to trough absorbances versus substrate concentration. Linear transformation of titration data was obtained by regression analysis.

Resonance Raman Measurements. The apparatus used to obtain resonance Raman spectra of NOS has been described in detail (*20*, *31*). Typically, a transparent rotating cell contained 100 μL samples of 20 μM nNOS, 1 mM imidazole, 4 μM H_4biopterin, and 3 mM DTT. The sample was irradiated at low laser power (0.3 mW) using an excitation wavelength of 406.7 nm, such that signals from both high-spin (Soret 395 nm) and low-spin (Soret 430 nm) hemes of Im−nNOS were able to be resonance enhanced. The scattered light spectra were baseline-corrected but unsmoothed. The frequencies of the Raman shift lines were calibrated against an indene standard. Absorption spectra of the samples were obtained in the sealed Raman cell (path length, 2 mm) before and after measuring the Raman spectra to ensure that the low-power laser excitation did not modify the enzyme.

Rapid Kinetic Measurements. All rapid kinetic measurements were obtained at 15 °C using a thermostated stopped-flow instrument obtained from Hi-Tech Ltd. (model SF-51). Experiments were performed by mixing a fixed amount of the Im−nNOS complex (0.5 μM initial concentration) with different concentrations of Arg or substrate analogues. Both sample and substrate were dissolved in Bis-Tris propane buffer, pH 7.6, containing 1 mM imidazole, 4 μM H_4-biopterin, and 0.5 mM DTT. The reaction was monitored by following the increase or decrease in absorbance at 390 or 427 nm, respectively. To determine the apparent rate constant, the time course for each kinetic experiment was fit to first-order exponential equations using a nonlinear least-squares method provided by the instrument manufacturer. The signal-to-noise ratios were improved by averaging 10 individual experiments.

RESULTS

Our nNOS preparation catalyzed initial rates of NO formation from homoArg, NMA, and NOHArg at initial rates of 630 (±25), 50 (±5), and 540 (±17) nmol/(min/mg of enzyme) at 37 °C, respectively, compared to a rate of 500 (±15) nmol/min per mg of enzyme from Arg. This confirmed that they serve as alternative substrates for nNOS (*33*). We next obtained spectral changes associated with binding of

[2] Because imidazole did not alter Arg binding affinity toward nNOS as determined under equilibrium conditions, this means that the free energy difference between Arg-free and Arg-bound states is unaffected. However, it cannot address whether the transition state for Arg binding is unaffected by imidazole.

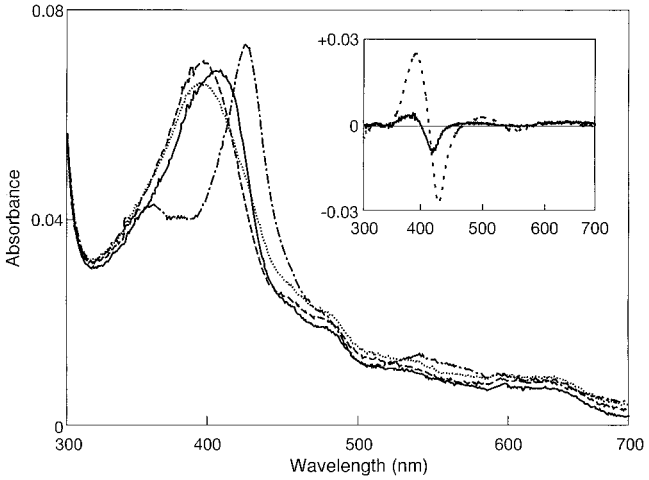

FIGURE 2: Spectral change upon binding Arg to nNOS in the presence or absence of imidazole. Consecutive spectra were obtained for H4biopterin-saturated nNOS in the absence (—) or presence (- - -) of 1 mM Arg. In a separate sample, consecutive spectra were recorded in the presence of 1 mM imidazole alone (- · -) and following addition of 1 mM Arg (···). The inset compares difference spectra generated by subtracting the spectrum of the Arg-free state from that of the Arg-replete state for the sample containing no imidazole (—) or containing 1 mM imidazole (- - -).

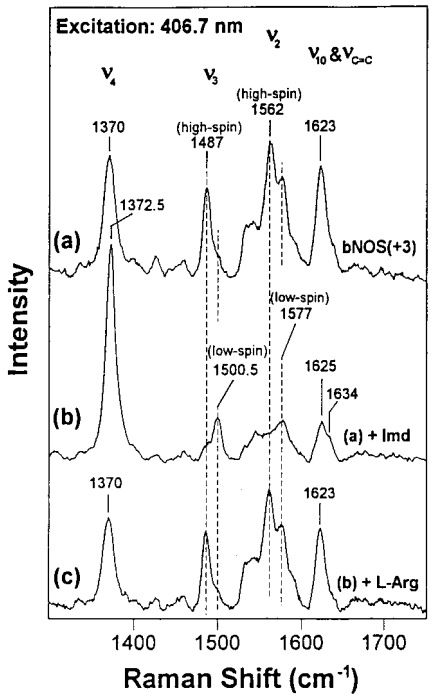

FIGURE 3: High-frequency resonance Raman spectra of nNOS and Im—nNOS. Trace A was obtained for 20 μM nNOS in 40 mM HEPES buffer pH 7.4, containing 20 μM H4biopterin. Spectrum B was obtained after adding 6 mM imidazole to the sample. Trace C was recorded after adding 8 mM Arg to the same sample. The samples were excited at 406.5 nm.

each substrate to nNOS in order to study their binding kinetics. However, addition of any substrate to H_4biopterin-saturated nNOS caused only a small change in absorption at 420 or 395 nm, owing to the predominantly high-spin state of H_4biopterin-saturated nNOS. Previous reports have demonstrated that Arg binding affinity toward H_4biopterin-saturated nNOS is unaffected by imidazole (*22*, *23*), and thus imidazole can be used to increase the degree of spectral change obtained with substrate binding. Figure 2 compares spectral changes obtained with our nNOS preparation upon binding Arg in the presence and absence of saturating imidazole. Arg binding to our Im—nNOS was also found to be independent of the imidazole concentration (data not shown). We therefore utilized Im—nNOS to study the kinetics of substrate binding.[2]

We initially employed resonance Raman spectroscopy to confirm that Arg binding to Im—nNOS releases imidazole from the heme and forms an nNOS—Arg complex. Spectra were obtained for nNOS and for Im—nNOS in the absence and presence of Arg. The spectrum of nNOS in the absence of Arg (Figure 3, trace A) confirmed it contains some ferric high-spin heme iron (*20*, *31*). Specifically, the spin-state marker line ν_3 is located at 1487 cm^{-1}, characteristic of high-spin heme iron (either five- or six-coordinate). Coordination of imidazole to substrate-free nNOS (Figure 3, trace B) resulted in a shift of ν_3 to 1500.5 cm^{-1}, indicating conversion to six-coordinate low-spin ferric heme. In addition, the frequency shifts of other marker lines such as ν_4, ν_2, and ν_{10} (see Table 1) and the intensification of ν_4 are all consistent with this assignment. Introduction of Arg to Im—nNOS (Figure 3, trace C) restored the high-spin heme spectral pattern, indicating that under this condition coordination of imidazole to the heme iron is prohibited by the binding of Arg.

We next studied substrate binding to Im—nNOS using stopped-flow spectroscopy. An absorbance decrease at 427 nm or increase at 400 nm were recorded upon mixing Im—nNOS with increasing amounts of substrate at 15 °C. The experiments were performed under pseudo-first-order conditions where substrate concentration was higher that the binding constant calculated by equilibrium spectral titration (see below) and much higher than the Im—nNOS concentration. In all cases, the kinetic traces of absorbance change during substrate binding to Im—nNOS were similar when measured at either wavelength and were best fit to a single-exponential equation. Figure 4 shows the time course for the reaction of Im—nNOS with two different concentrations of Arg when monitored at 427 nm. Both signals exhibited first-order kinetics and when fit to a single-exponential equation gave observed rate constants of 2.7 and 70 s^{-1}, respectively. Figure 5 contains plots of observed rate constant versus substrate concentration for each of the four substrates used in this study. Saturation kinetics were obtained for all substrates.[3] The kinetic values for each substrate were derived from the graphs and are listed in Table 2.

Table 1: Resonance Raman Marker Lines (in cm^{-1}) for High- or Low-Spin Heme Ferric nNOS

	ν_4	ν_3	ν_2 (ν_{11}, ν_{37})	ν_{10} ($\nu_{C=C}$)
high-spin (5- or 6-coordinate)	1370	1487	1562	1623
low-spin (6-coordinate)	1372.5	1500.5	1577	1634

Spectral binding constants (K_s) for the four substrates were also derived by equilibrium titration of the low-spin Im—nNOS complex with increasing concentrations of each

[3] This may distinguish nNOS from eNOS, whose Arg binding did not appear to exhibit saturation kinetics (*30*).

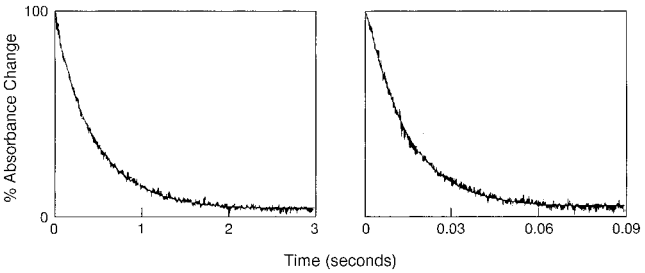

FIGURE 4: Time course of spectral change associated with Arg binding to Im−nNOS at 15 °C. The nNOS (1 μM) in the presence of 1 mM imidazole was mixed rapidly with 50 μM Arg (left panel) or 6 mM Arg (right panel), and the progress of the reaction was monitored at 427 nm. The solid line drawn through each experimental trace is the curve of the best fit described by a single-exponential equation ($y = Ae^{-k_1 t} + C$).

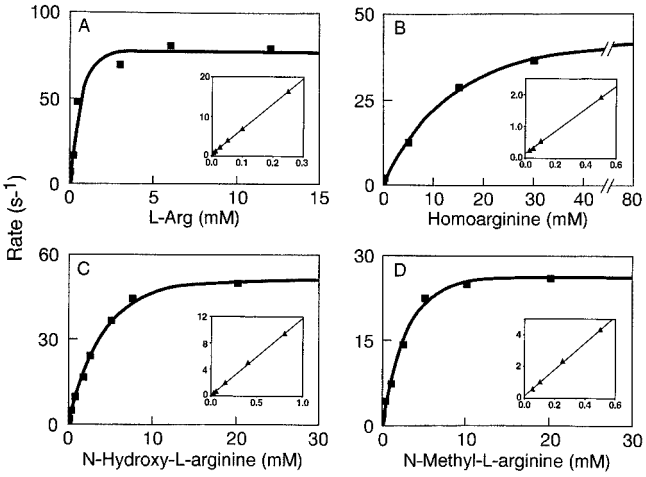

FIGURE 5: Pseudo-first-order rate constants of spectral change observed upon substrate binding to Im−nNOS plotted versus substrate concentration. The insets show data obtained at the lower substrate concentrations. The *y* intercepts provide an estimate of k_{-2} values and were derived by linear regression analysis of the inset data (solid lines).

Table 2: Kinetic Parameters Calculated for Substrate Binding to nNOS Using Pre-Steady-State (Stopped-Flow) or Equilibrium Methods

substrate	K_{-1} (mM)	k_2 (s^{-1})	k_{-2} (s^{-1})	K_s (μM)	K_s[a]	K_m[b]
Arg	0.5	81	0.45	3	3	4
homoArg	10	42	0.2	48	50	57
NOHArg	2.7	57	0.07	3	1	25[c]
NMA	1.7	27	0.2	12	2	3[d]

[a] Determined by the equilibrium spectral titration method. [b] Determined by measuring steady-state rates of NO or citrulline synthesis. [c] From ref 42. [d] For mouse iNOS from ref 35.

substrate, as done previously for Arg and NOHArg (*23*). The equilibrium K_s values are listed in Table 2, along with K_m values determined for each substrate using the oxyhemoglobin NO synthesis assay.

DISCUSSION

Substrate Interaction with nNOS and Capacity To Support NO Synthesis. In this report we utilized stopped-flow and equilibrium methods to characterize the mechanism of substrate binding to nNOS. Although all four substrates we used shifted the nNOS heme iron spin equilibrium toward high spin upon binding, some of the substrates have somewhat different effects on heme iron electronic and coordination properties (*17*). They also differ in their capacity to act as substrates for NO synthesis. For example, conversion of either Arg or NOHArg to NO is tightly coupled to nNOS NADPH oxidation (*10*, *33*). In contrast, NO production from homoArg or NMA is partially or highly uncoupled from enzyme NADPH oxidation, respectively, and NMA metabolism is associated with time-dependent heme destruction and irreversible loss of nNOS enzyme activity (*34*). Uncoupling and eventual enzyme inactivation during NMA oxidation is due in part to NMA requiring oxidative N-demethylation prior to or following N-hydroxylation in order to generate NO (*35*).

All four substrates we tested contain a guanidino moiety. In recent crystal structures of NOS oxygenase domains (*14*−*16*), an Arg guanidino bridging nitrogen and terminal nitrogen form hydrogen bonds with the carboxylate moiety of a conserved glutamate residue that is located in the distal heme pocket. Mutagenesis and substrate analogue studies indicate that these hydrogen-bonding interactions are critical for high affinity binding and possibly for NO synthesis (*36*−*38*). The hydrogen-bonding arrangement positions the substrate's free guanidino nitrogen above the heme iron, presumably to react with heme-bound activated oxygen. Thus, spectral changes seen upon substrate binding to Im−nNOS likely reflect conformational and electronic changes in the heme pocket associated with enzyme−substrate hydrogen bond formation and expulsion of imidazole from the heme iron.

Kinetics of Substrate Binding. In general, substrate binding can occur in a single step or can follow a two or more step mechanism (*32*). A one step mechanism will result in an ever-increasing apparent rate of binding as substrate concentration increases. In contrast, a two or more step mechanism will result in an increasing apparent rate of binding that reaches a maximum at some finite substrate concentration. In such cases, the rate obtained at saturation is governed by the first-order reversible transformation of an ES to E′S complex (*32*). In all cases a number of kinetic parameters and the overall binding constant can be determined from the kinetic data.

Because rebinding of imidazole to nNOS is negligible when substrate concentrations are well above the substrate K_s (*23*), we were able to directly determine rates of substrate binding from the spectral change that accompanies conversion of Im−nNOS to its imidazole-free, substrate-bound form. For each substrate tested, the apparent rate for binding approached or achieved a maximal value at higher substrate concentrations. In addition, for any given substrate or concentration the spectral changes versus time traces were best fit to a single-exponential equation, indicating a monophasic transition was occurring in all cases. As summarized in Scheme 1, these kinetic features suggest that substrate binding to nNOS is a two-step reversible reaction in which there is a rapid binding equilibrium between Im−nNOS and the substrates (S) to form an intermediate that contains bound imidazole and substrate. Both the initial and intermediate species display the same spectrum. This is followed by a slower conformational change in the Im−enzyme−substrate complex that is associated with release of bound imidazole, a shift in the spectrum, and generation of a modified

enzyme−substrate complex (nNOS′−S) that forms in a unimolecular and reversible process from the intermediate:

Scheme 1

$$\text{Im}-\text{nNOS} + \text{S} \underset{k_{-1}}{\overset{k_1}{\rightleftharpoons}} \text{Im}-\text{nNOS}-\text{S} \underset{k_{-2}}{\overset{k_2}{\rightleftharpoons}} \text{Im} + \text{nNOS}'-\text{S}$$

A similar conformational change in iNOS or nNOS dimers has also been proposed to explain expulsion of the heme ligands DTT (*27*, *28*) or water (*26*, *27*, *39*) upon binding H_4biopterin or Arg.

Analysis of the kinetic graphs in Figure 5 provide estimated values for K_{-1}, k_2, k_{-2}, and the binding constant K_s. At saturating levels of substrate, the maximal rate of the reaction is equal to the sum of k_2 and k_{-2}, while the *y*-intercept represents k_{-2}. The constant K_{-1} is equal to the substrate concentration at which half the saturation rate is achieved and is also equivalent to k_{-1}/k_1 (*32*). The overall binding constant (dissociation constant) for the neuronal NOS−substrate interaction can be described by the following equation (*32*):

$$K_s = \frac{K_{-1}}{1 + (k_2/k_{-2})}$$

Binding constants derived from kinetic analysis of each substrate are listed in Table 2 along with binding constants derived from equilibrium spectral binding measurements. In general, there is very good agreement between K_s values derived from the stopped-flow versus equilibrium studies, except for NMA.

The kinetic analysis is valuable because it can reveal a basis for divergent enzyme response to different substrates. For example, a comparison of the kinetic parameters for homoArg and Arg shows that their distinct binding affinities arise from kinetic differences in both steps of the substrate binding reaction. The four substrates we tested clearly display different maximal binding rate constants at high substrate concentrations (see Figure 5). Arg has the fastest maximal rate, which is approximately two times greater than that observed for homoArg or NOHArg and is four times greater than that observed for NMA. Because the estimated k_{-2} values are relatively slow for all four substrates (see Table 2), the different maximal rate values primarily reflect differences in the estimated value of k_2 for each substrate. This implies that the rate of the nNOS−S to nNOS′−S transition can differ markedly depending on substrate structure. This is consistent with EPR work showing that Arg, NOHArg, and NMA each generate a distinct class of high-spin complex after binding to nNOS (*17*, *40*) and to the other NOS isoforms (*20*, *26*, *31*, *33*, *39*, *41*). It is presently unclear how the rate of the nNOS−S to nNOS′−S transition (k_2) determines a compound's ability to modify heme iron reactivity, alter enzyme NADPH oxidation, and serve as a substrate for NO synthesis. However, our current data suggest that a slow k_2 value might hinder a substance's ability to function as a substrate in a coupled manner, as is the case for NMA. The stopped-flow kinetic analysis as described here can be expanded to study binding of substrate-based inhibitors and compare nNOS mutants in structure−function analysis.

ACKNOWLEDGMENT

We thank Pam Clark for excellent technical assistance.

REFERENCES

1. Ignarro, L. J. (1990) *Annu. Rev. Pharmacol. Toxicol. 30*, 535−560.
2. Moncada, S., Palmer, R. M. J., and Higgs, E. A. (1991) *Pharmacol. Rev. 43*, 109−142.
3. Schmidt, H. H. H. W., and Walter, U. (1994) *Cell 79*, 919−925.
4. Vincent, S. R. (1994) *Prog. Neurobiol. 42*, 129−160.
5. Mayer, B., and Henmens, B. (1997) *Trends Biochem. Sci. 22*, 477−481.
6. McMillan, K., Bredt, D. S., Hirsch, D. J., Snyder, S. H., Clark, J. E., and Masters, B. S. S. (1992) *Proc. Natl. Acad. Sci. U.S.A. 89*, 11141−11145.
7. Stuehr, D. J., and Ikeda-Saito, M. (1992) *J. Biol. Chem. 267*, 20547−20550.
8. Abu-Soud, H. M., and Stuehr, D. J. (1993) *Proc. Natl. Acad. Sci. U.S.A. 90*, 10769−10772.
9. Abu-Soud, H. M., Yoho, L. L., and Stuehr, D. J. (1994) *J. Biol. Chem. 269*, 32047−32050.
10. Abu-Soud, H. M., Feldman, P. L., Clark, P., and Stuehr, D. J. (1994) *J. Biol. Chem. 269*, 32318−32326.
11. Abu-Soud, H. M., Gachhui, R., Raushel, F. M., and Stuehr, D. J. (1997) *J. Biol. Chem. 272*, 17349−17353.
12. Marletta, M. A. (1993) *J. Biol. Chem. 268*, 12231−12234.
13. Sono, M., Stuehr, D. J., Ikeda-Saito, M., and Dawson, J. H. (1995) *J. Biol. Chem. 270*, 19943−19948.
14. Crane, B. R., Arvai, A. S., Gosh, D. K., Wu, C., Getzoff, E. D., Stuehr, D. J., and Tainer, J. A. (1998) *Science 279*, 2121−2126.
15. Raman, C. S., Li, H., Martasek, P., Kral, V., Masters B. S. S., and Poulos, T. M. (1998) *Cell 95*, 939−950.
16. Fischmann, T. O., Hruza, A., Niu, X. D., Fossetta, J. D., Lunn, C. A., Dolphin, E., Prongay, A. J., Reichert, P., Lundell, D. A., Narula, S. K., and Weber, P. C. (1999) *Nat. Struct. Biol. 6*, 233−242.
17. Salerno, J. C., Fery, C., McMillan, K., Williams, R. F., Masters, B. S. S., and Griffith O. W. (1995) *J. Biol. Chem. 270*, 27423−27428.
18. Presta, A., Weber-Main, A. M., Stankovich, M. T., and Stuehr, D. J. (1998) *J. Am. Chem. Soc. 120*, 9460−9465.
19. Abu-Soud, H. M., Wu, C., Ghosh, D. K., and Stuehr, D. J. (1998) *Biochemistry 37*, 3777−3786.
20. Wang, J., Rousseau, D. J., Abu-Soud, H. M., and Stuehr, D. J. (1994) *Proc. Natl. Acad. Sci. U.S.A. 91*, 10512−10516.
21. Matsuoka, A., Stuehr, D. J., Olson, J. S., Clark, P., and Ikeda-Saito, M. (1994) *J. Biol. Chem. 269*, 20335−20339.
22. Wolf, D. J., Datto, G. A., Samatovicz, R. A., and Tempsick, R. A. (1993) *J. Biol. Chem. 268*, 9425−9429.
23. McMillan, K., and Masters, B. S. S. (1993) *Biochemistry 32*, 9875−9880.
24. Hurshman, A. R., and Marletta, M. A. (1995) *Biochemistry 34*, 5627−5634.
25. Scheele, J. S., Kharitonov, V. G., Martasek, P., Roman, L. J., Sharma, V. S., Masters, B S. S., and Magde, D. (1997) *J. Biol. Chem. 272*, 12523−12528.
26. Wang, J., Stuehr, D. J., and Rousseau, D. L. (1997) *Biochemistry 36*, 4595−4606.
27. Ghosh, D. K., Wu, C., Pitters, E., Moloney, M., Werner, E. R., Mayer, B., and Stuehr, D. J. (1997) *Biochemistry 36*, 10609−10619.
28. Gorren, A. C. F., Schrammel, A., Schmidt, K., and Mayer, B. (1997) *Biochemistry 36*, 4360−4366.
29. McMillan, K., and Masters, B. S. S. (1995) *Biochemistry 34*, 3686−3693.
30. Berka, V., Chen, P., and Tsai, A. (1996) *J. Biol. Chem. 271*, 33293−33300.
31. Wang, J., Stuehr, D. J., Ikeda-Saito, M., and Rousseau, D. L. (1993) *J. Biol. Chem. 268*, 22255−22258.
32. Hiromi, K. (1979) *Kinetics of Fast Enzyme Reactions: Theory and Practice*, Halsted Press Book, Kodansha Ltd., Tokyo.

33. Sennequier, N., and Stuehr, D. J. (1996) *Biochemistry 35*, 5883−5892.
34. Olken, N. M., Osawa, Y., and Marletta, M. A. (1994) *Biochemistry 33*, 14784−14791.
35. Olken, N. M., and Marletta, M. A. (1993) *Biochemistry 32*, 9677−9685.
36. Gachhui, R., Ghosh, D. K., Wu, C., Parkinson, J., Crane, B. R., and Stuehr, D. J. (1997) *Biochemistry 36*, 5097−5103.
37. Chen, P.-F., Tsai, A.-L., Berka, V., and Wu, K. K. (1997) *J. Biol. Chem. 272*, 6114−6118.
38. Martasek, P., Miller, R. T., Liu, Q., Roman, L. J., Salerno, J. C., Migita, C. T., Raman, C. S., Gross, S. S., Ikeda-Saito, M., and Masters, B. S. S. (1998) *J. Biol. Chem. 273*, 34799−34805.
39. Wang, J., Stuehr, D. J., and Rousseau, D. L. (1995) *Biochemistry 34*, 7080−4087.
40. Salerno, J. C., Martasek, P., Roman, L. J., and Masters, B. S. S. (1996) *Biochemistry 35*, 7626−7630.
41. Salerno, J. C., Martasek, P., Williams, R. F., and Masters, B. S. S. (1997) *Biochemistry 36*, 11821−11827.
42. Klatt, P., Schmidt, K., Uray, G., and Mayer, B. (1993) *J. Biol. Chem. 268*, 14781−14787.

BI990698X